



OPEN Identification and quantification of muscular cocontraction for ankle rehabilitation through variational mode decomposition in surface electromyography

Sania Yasmeen¹, Asim Waris¹, Faisal Amin¹, Javaid Iqbal¹, Syed Omer Gilani², Muhammad Jawad Khan^{3✉}, Fawwaz Hazzazi³, Ahmed Imran⁴, Umer Hameed Shah⁴ & Muhammad Adeel Ijaz⁵

The ankle joint plays important role in performing fundamental activities such as walking and other essential daily tasks. Ankle stabilization and muscle co-contraction are crucial for rehabilitating gait abnormalities, as impaired ankle function disrupts gait, causes pain and inflammation, and hampers recovery. Accurate assessment of muscle co-contraction is crucial for developing effective non-pharmacological interventions. This paper introduces a novel approach using Variational Mode Decomposition (VMD) combined with scalogram visualization technique to analyze surface electromyographic (sEMG) signals from antagonist muscles of the lower limb and assesses muscular co-contraction using the coscalogram function. The present study compares VMD with the Continuous Wavelet Transform (CWT) approach and shows that VMD outperforms CWT in terms of both SNR and RMSE. On average, the increase in SNR in case of VMD ($-17.65 \pm 8.1\text{dB}$ to $2.98 \pm 2.2\text{dB}$) was greater than that of CWT ($-17.65 \pm 3.7\text{dB}$ to $1.34 \pm 1.5\text{dB}$). Similarly, the reduction in RMSE with VMD (0.023 ± 0.0029 to 0.017 ± 0.0015) surpassed that achieved with CWT (0.023 ± 0.0027 to 0.020 ± 0.0025). This enhanced accuracy in identifying co-contraction events has the potential to significantly improve clinical assessment and rehabilitation strategies for patients with ankle joint pathologies. To further validate VMD's effectiveness, we quantitatively assessed co-contraction events by comparing mean peak amplitudes identified using VMD and CWT. Our analysis, which revealed that VMD consistently captured stronger co-contraction events (higher mean peak amplitudes), supports VMD's superiority in accurately identifying and quantifying ankle muscle co-contraction. These results have significant implications for clinical practice, offering the potential for more precise assessments of ankle joint function and the development of more targeted and effective rehabilitation interventions.

Keywords Variational mode decomposition, Scalogram, sEMG, Co-contraction, Continuous wavelet transform, Ankle rehabilitation

Electromyography (EMG) measures how accurately our muscles respond to nerve signals from the brain by evaluating and recording the electrical activity of muscles. EMG signals play an important role in clinical/medical and engineering fields. They are of two types: surface electromyography (sEMG) and intramuscular EMG¹. Both differ from each other by electrodes i.e. non-invasive and invasive electrodes². sEMG is preferably used nowadays to extract information about muscle activation³. EMG signals can be used to diagnose nerve

¹Department of Biomedical Engineering and Sciences, School of Mechanical and Manufacturing Engineering, National University of Sciences and Technology (NUST), Islamabad, Pakistan. ²Department of Electrical, Computer, and Biomedical Engineering, Abu Dhabi University, Abu Dhabi, UAE. ³Department of Electrical Engineering, College of Engineering, Prince Sattam bin Abdulaziz University, 11942 Al-Kharj, Saudi Arabia. ⁴Department of Biomedical Engineering & Artificial Intelligence Research Center, College of Engineering and Information Technology, Ajman University, Ajman, UAE. ⁵Department of Biomedical Engineering and Sciences, School of Mechanical and Manufacturing Engineering (SMME), National University of Sciences and Technology (NUST), Islamabad, Pakistan. ✉email: mt.khan@psau.edu.sa

damage, muscle dysfunction, etc. Furthermore, they can be used for rapid torque development⁴, gait analysis, and recording muscle movements e.g. muscle co-contraction⁵. For this purpose, the acquisition of an accurate EMG signal is essential^{6,7}.

Muscle co-contraction refers to the simultaneous activation of antagonist muscles around a joint. It's a normal motor control strategy that aids in performing several functional tasks. During limb movement, muscle co-contraction results in joint stiffness, hence enhancing the stability and accuracy of the joint⁸. Walking at various speeds and over greater distances/durations would increase muscle co-contraction recruitment and subject variability⁹. Excessive co-contraction is a major contributing factor to walking impairments¹⁰, causes fatigue¹¹, increases energy expenditure, and may impede movement¹². Muscular co-contraction is hypothesized to be a good application for clinical purposes. Different techniques have been introduced to evaluate muscular co-contraction, but a gold standard has not yet been established. Previous studies have demonstrated that various techniques have been adopted for the analysis of muscle co-contraction of sEMG signals taken from the upper limb i.e. Co-contraction Index (CCI)⁸, Double threshold statistical algorithm (DT)¹³, Rudolph's index (RI)¹⁴ etc. However, there is a lack of information on lower limb¹⁵ muscle co-contraction during walking. Recently, a group of researchers presented a comprehensive analysis of thigh muscle¹⁶ and ankle muscle co-contraction¹⁷. Researchers have designed various studies, but due to poor decomposition performance, instability, modal aliasing effect, and low noise resistance, the efficacy of ankle muscle co-contraction to be helpful for joint health remains unclear, along with the evidence of ankle muscle co-contraction to be advantageous for rehabilitation purpose required improvement.

The need is to characterize the ankle muscle co-contraction in sEMG signal by using an efficient technique to make sure that it could be a non-pharmacological treatment for persons having ankle joint issues¹⁸. For this purpose, the present work will focus on Variational Mode Decomposition (VMD), a signal processing technique that decomposes the input signal into different band-limited intrinsic mode functions (IMFs)¹⁹, proposed by Dragomiretskiy et al. in 2013²⁰. The method can perfectly reconstruct the original signal from its smoothed decomposed in IMFs after demodulation into the baseband, making it robust to sampling and noise²¹. This advantage enhances its utility in various fields such as speech signal processing²², signal denoising^{23–25}, fault diagnosis^{26,27}, and seismic time-frequency analysis²⁸. VMD provides improvement over other techniques such as no modal aliasing effect²⁹, better decomposition performance, stability, and sensitivity to noise. Although VMD had been used previously for different purposes but it's being used for this purpose first time.

This study is designed to assess the appropriate detection of ankle muscle co-contraction in healthy adults for clinical interpretation of the role of muscular co-contraction and control, and stabilization of ankle joint in clinical environment. To this aim, the Tibialis Anterior (TA) and Gastrocnemius Lateralis (GL) were selected as representative muscles of the ankle. In this study, VMD is compared with CWT approach only, not other denoising techniques like empirical mode decomposition, discrete wavelet transforms etc. because until now only CWT has been used as a decomposition technique for this purpose. In future, other denoising methods may be used. This study aims to introduce a better method that would be helpful for clinical and rehabilitation purposes to improve joint quality by identifying ankle muscle co-contraction accurately using the novel combination of scalogram visualization technique with VMD for the first time.

Methods

Subjects

The dataset contains sEMG signals collected during the walking of 20 healthy adults (10 females and 10 males). Mean (\pm Standard Deviation, SD) characteristics are age 24 ± 2 years; height 172 ± 10 cm; weight 62 ± 8 kg; Body mass index (BMI) 21.5 ± 2.1 kg/m². Exclusion criteria include pathological or chronic joint pain, abnormal gait, surgical intervention, and BMI ≥ 25 . The other (online) walking dataset of 5 healthy subjects is taken from UCI Machine Learning Repository (O Sanchez et al., 2014). In the online dataset, each trial had a signal acquisition duration of 10 s. The signals were recorded under controlled conditions with standardized ankle movements. Data was acquired with a sampling rate of 1000 Hz to ensure high-resolution muscle activity measurements. Informed consent was obtained before the experiment from all subjects involved in this study. Approval (Ref # NUST/SMME-BME/ REC/000142/20012023) was granted by the local ethical committee of the National University of Science and Technology and accomplished according to the institutional regulations and principles of the Declaration of Helsinki. This study focused on healthy participants due to ethical constraint.

Experimental setup

Delsys Trigno Wireless EMG Sensors were used for data collection from lower limb muscles. Firstly, the targeted muscle area was cleaned with an alcohol swab, and excess hair was shaved. Before electrode placement, it was important to ensure that the skin surface above the muscles was clean for proper electrode-skin contact. sEMG electrodes were placed on the skin surface above the muscle belly of the muscle. The shin muscles used for data collection were TA and GL as they were selected as representative muscles of the ankle. The GL was selected as a representative of the gastrocnemius muscle group due to its accessibility for surface EMG and its established role in ankle plantarflexion, which is crucial for walking.

Signal acquisition and processing

To record muscle activity, two (2) wireless surface EMG sensors (Trigno Wireless EMG system, Delsys, Boston, MA, USA) were positioned on ankle muscles according to SENIAM (Surface Electromyography for the Non-Invasive Assessment of Muscles) recommendations [30]. sEMG signals were measured during 30 s of ground walking. The experimental setup is shown in Fig. 1. Subjects were instructed to walk on a flat surface for a period of 30 s at their usual pace. The natural pace was selected because walking at a comfortable speed enhances the consistency of EMG data, whereas variability increases when subjects are asked to walk abnormally³⁰.

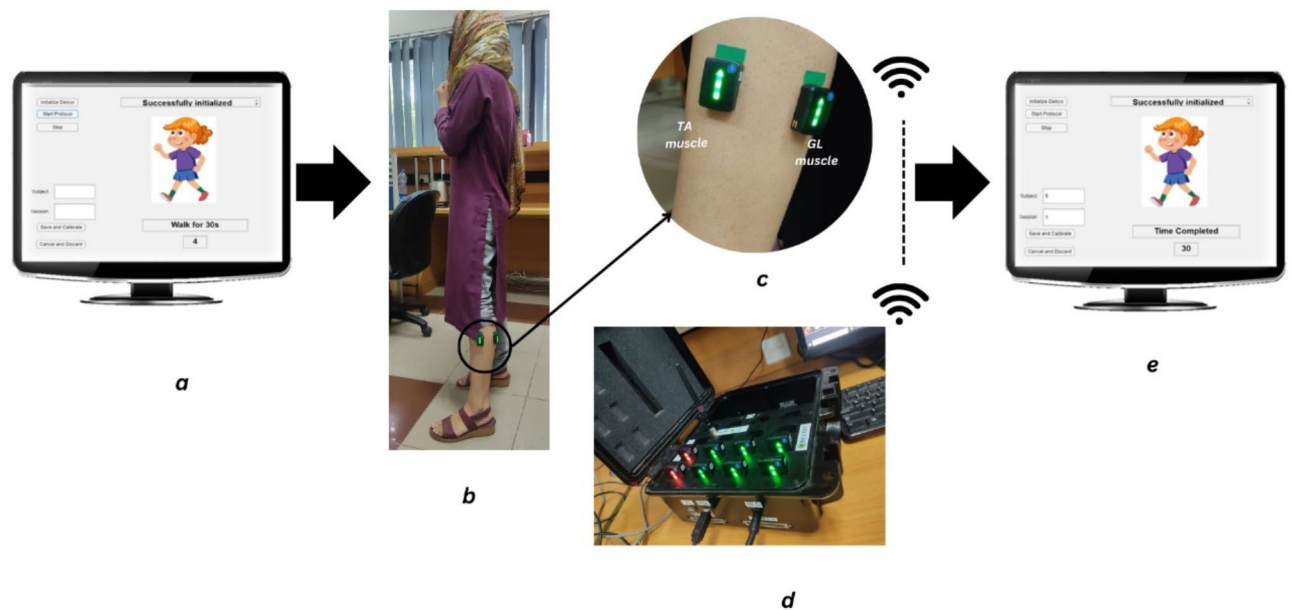


Fig. 1. Experimental Setup (a) Data protocol starts, as Delsys successfully initiated (b) Subject providing data (c) Electrode placement on Tibialis Anterior (TA) and Gastrocnemius Lateralis (GL) muscles of lower limb (d) sEMG acquisition system (e) Protocol ends after data collection.

Data collection, preprocessing of data was carried out. Recorded data from sEMG signals were filtered by applying Butterworth 4th order bandpass filter, with lower and upper cut-off frequencies 20 Hz and 500 Hz respectively, to remove any undesired frequency content. To reduce power line interference, the sEMG signals were filtered using a notch filter with a 60 Hz cutoff frequency. After that, VMD was adopted to efficiently denoise the signal. VMD decomposes EMG data into a set of simpler components known as modes or IMFs. Research by Xiao et al. provides the mode selection criteria and shows that VMD has large potential to denoise EMG signals³¹.

Each mode represents a distinct component or pattern in the EMG signal. These patterns, as displayed in Fig. 2, correspond to muscle-relevant information e.g. muscular activity, or irrelevant information e.g. noise or artifact. These modes are refined iteratively by updating their parameters in each iteration³². This involves a two-step process: first, the modes are updated in the frequency domain, adjusting their central frequencies based on the signal's spectral content. Then, in the time domain, the modes are refined by minimizing the interference between them.

The frequency spectrum shows that each IMF contains a central frequency and a narrow frequency band³³ as illustrated in Fig. 3. Finally, IMF components with narrow bands were extracted based on the frequency domain characteristics of the signal³¹. Each IMF is updated with every iteration. Thus, minimizing noise iteratively. This study focuses on elucidating the distinct advantages of VMD, specifically in its utilization of iterative processes within the intrinsic mode functions (IMFs), resulting in more effective noise reduction compared to the conventional CWT. CWT lacks this intrinsic property of iterative refinement of IMFs. These decomposed models containing significant data are combined to reconstruct the original signal. Reconstructed signal represents the essential features of muscle activity while minimizing noise and artifacts. The overall stepwise methodology is displayed in Fig. 4.

Subsequently, the scalogram function was employed to evaluate muscular activation. Scalogram visualization techniques have always been used with wavelet transform in the past^{17,34}. In this research, it is used with VMD for the first time. Scalogram represents energy localization in the time-frequency domain¹³. Using the Scalogram visualization technique with VMD helps gain insights into the time-frequency characteristics of the signal's intrinsic mode functions.

The coscalogram function of denoised sEMG signals offers a quantitative approach for assessing the co-contraction between muscles. The onset and offset of co-contraction activity were determined by identifying the start and end points of the energy zones in the coscalogram. Furthermore, quantitative assessment of the co-contraction events was carried out to demonstrate the

effectiveness of VMD compared to CWT. The 'findpeaks' function was used to identify prominent co-contraction events in the co-scalograms generated by both VMD and CWT. The peak amplitudes for the identified co-contraction events in both the VMD and CWT co-scalograms were then extracted. Next, the mean of these peak amplitudes for each technique was calculated to obtain a representative value of co-contraction intensity. Finally, the mean peak amplitudes between VMD and CWT were compared to determine which method more effectively captures stronger co-contraction events. The Fig. 5 shows the steps that are carried out for quantitative assessment of muscular co-contraction.

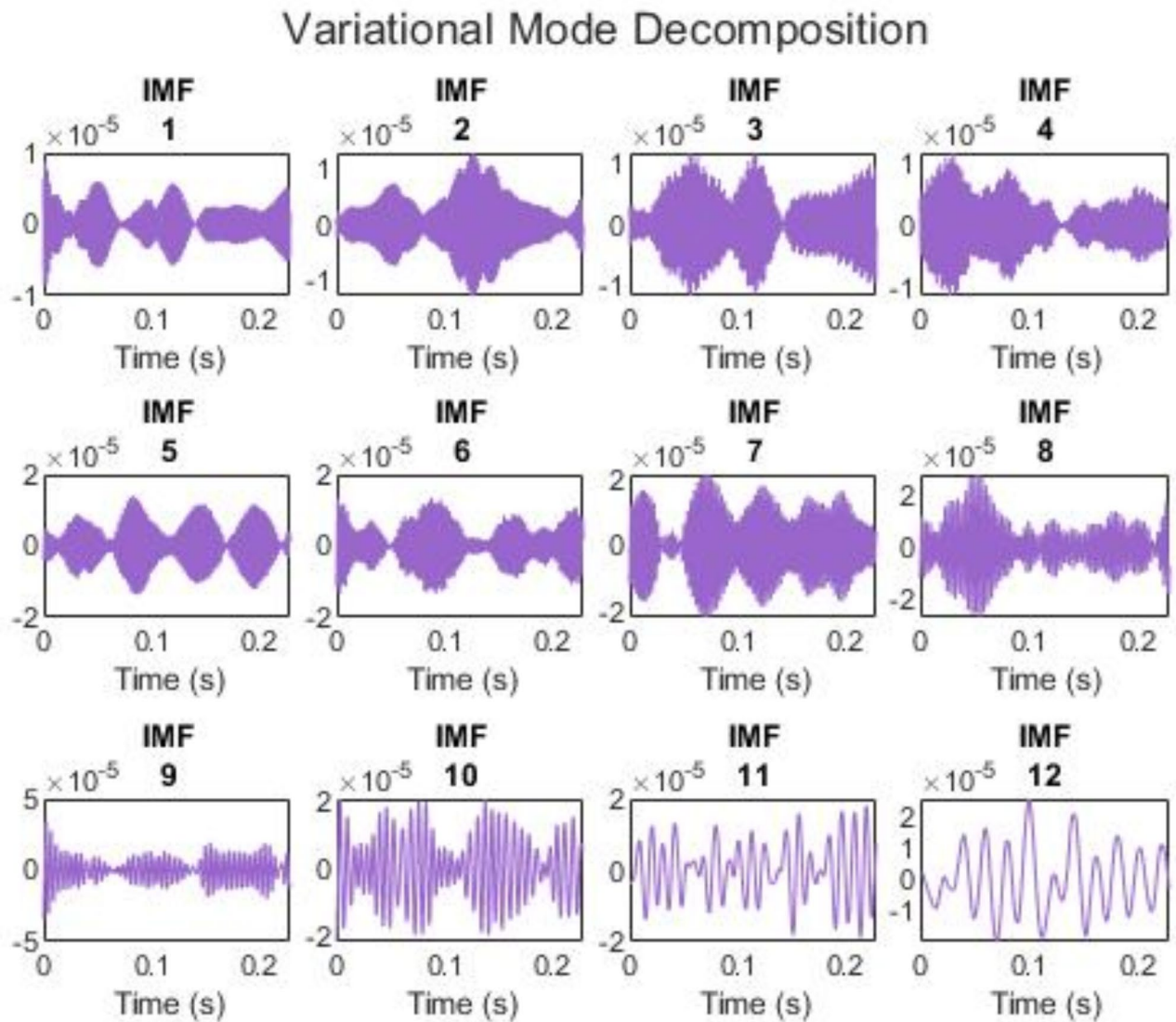


Fig. 2. Decomposition of sEMG signal using VMD. The original sEMG signal is decomposed into multiple Intrinsic Mode Functions (IMFs), each representing a specific frequency band.

Evaluation parameters

To evaluate the denoising effect, the variational mode decomposition method is compared with the traditional wavelet method (CWT). In addition, the signal-to-noise ratio (SNR) and root mean square error (RMSE) between the denoising sEMG signal and the original signal are calculated. The corresponding Eq. (1) and Eq. (2) are below:

$$SNR = 10 \cdot \log_{10} \left(\frac{\sum (f^2)}{\sum ((f - \hat{f})^2)} \right) \quad (1)$$

$$RMSE = \sqrt{\frac{1}{L} \sum (f - \hat{f})^2} \quad (2)$$

where f is the original signal and \hat{f} is the denoised signal and L is the length of the signal.

Statistical analysis

The results obtained were validated by comparing the SNR and RMSE of all three groups (raw data, CWT-processed data, VMD-processed data) collectively using the ANOVA test. A significant difference ($p < 0.05$) was determined through the ANOVA one-way testing.

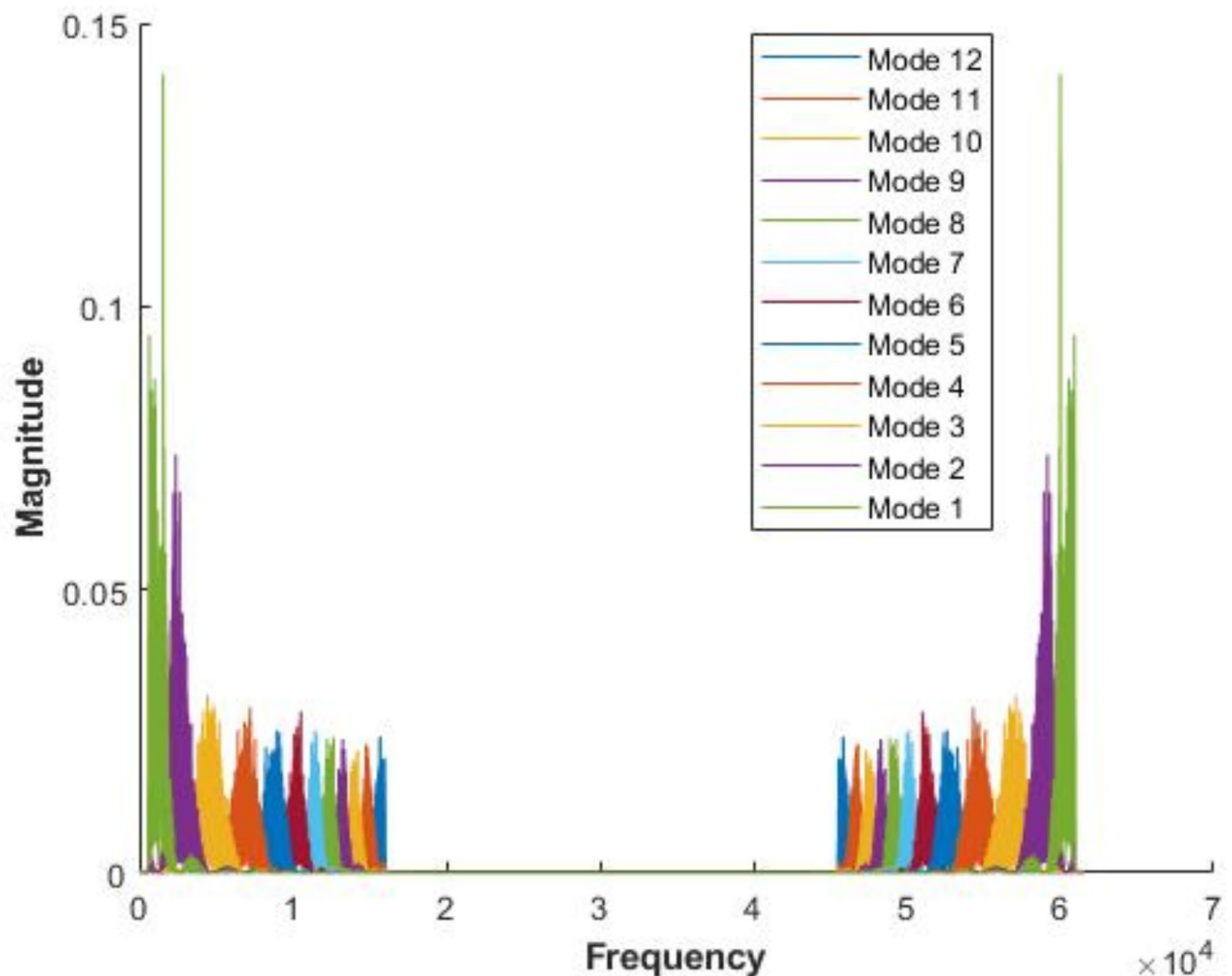


Fig. 3. Frequency spectrum of IMFs obtained by VMD. The first IMF contains the highest frequency range and thus the most amount of noise, while subsequent IMFs represent progressively lower frequency components with reduced noise. This spectral distribution highlights the effectiveness of VMD in decomposing the sEMG signal into distinct frequency bands for analysis.

Results

The VMD technique was applied to sEMG data from 20 subjects, decomposing the signal into multiple IMFs. The significant data in the decomposed models are merged to reconstruct the original signal. In Fig. 6, a comparison between the original signal and the signal after denoising can be clearly seen. The signal has retained its original characteristics while minimizing the noise. The results illustrated in Figs. 7 and 8 demonstrate a notable enhancement of SNR and a significant reduction in RMSE respectively, of TA and GL muscles after applying VMD. These outcomes strongly indicate the efficacy and suitability of the VMD technique. A higher SNR and lower RMSE indicate better noise reduction while preserving important signal features³³. After obtaining promising outcomes through the application of the VMD, a comparative assessment was conducted with the Continuous Wavelet Transform (CWT) technique to discern their relative effectiveness. SNR results displayed in Fig. 9, and RMSE results in Fig. 10 showed a noticeable discrepancy between VMD and CWT in terms of their noise reduction capabilities.

The iterative nature of VMD in generating IMFs demonstrated a marked reduction in noise levels, underscoring its superiority over CWT. The absence of an iterative process in CWT hindered its ability to achieve comparable levels of noise reduction. To further reinforce the findings, the process was repeated using online data. This extended evaluation consistently affirmed VMD's superior performance over CWT. The comparison of results obtained after applying CWT and VMD on online data as well as offline data illustrated improvement in SNR in Fig. 11 and minimization in RMSE in Fig. 12. The results demonstrate that VMD outperforms CWT in terms of both SNR and RMSE. Furthermore, quantitative assessment of the co-contraction events was carried out by comparing the mean peak amplitudes of VMD and CWT to demonstrate the effectiveness of VMD compared to CWT. Table 1 shows the mean peak amplitude values obtained from the VMD co-spectrogram in every segment is substantially higher than the mean peak amplitude obtained from the CWT co-spectrogram.

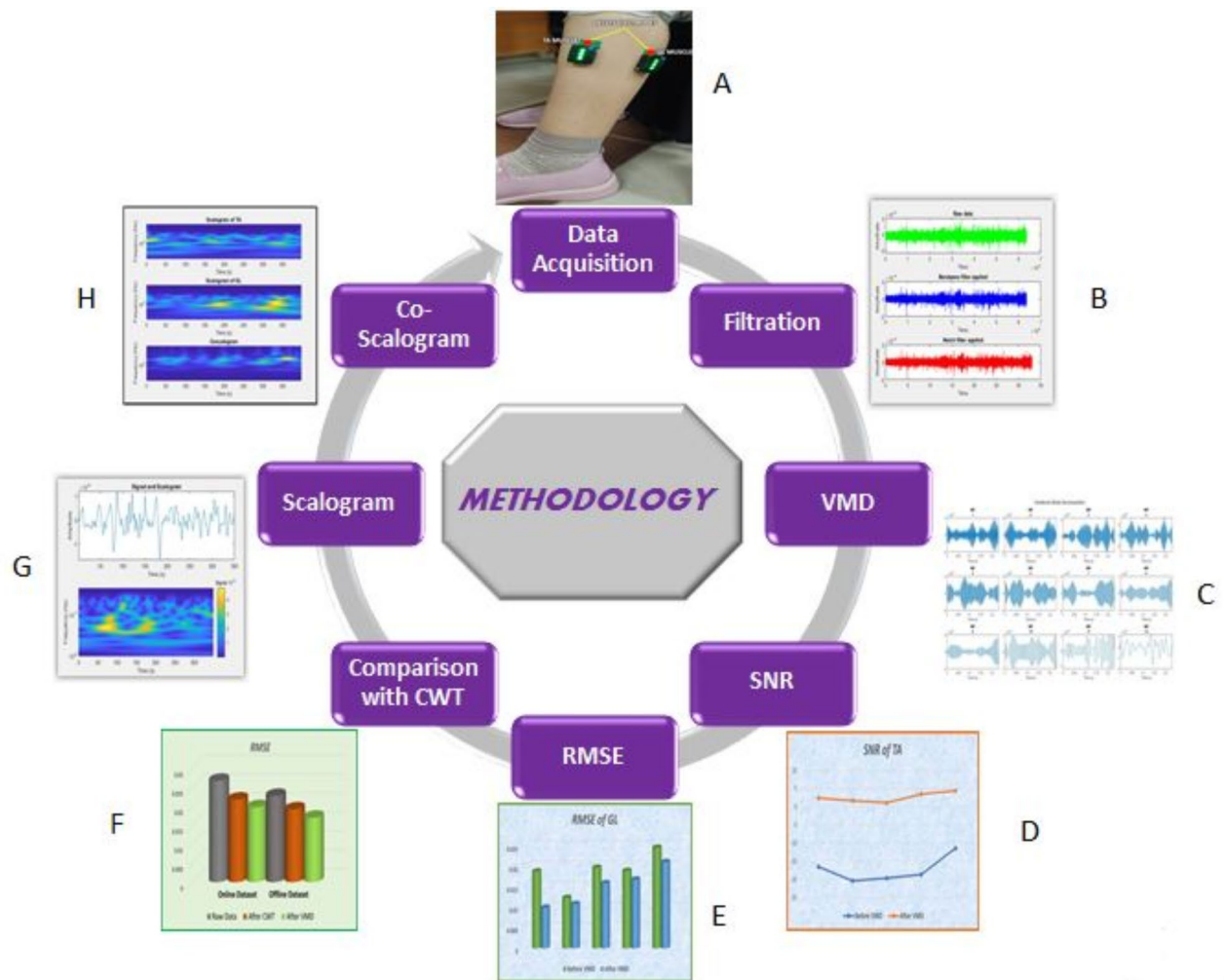


Fig. 4. Methodology (A) Acquire the raw data through Delsys trigno wireless EMG sensors. (B) Apply a filtration process to remove unwanted noise or interference from the acquired data. (C) Utilize Variational Mode Decomposition (VMD) to decompose the signal into its constituent components. (D) Evaluate the Signal-to-Noise Ratio (SNR) to quantify the quality of the decomposed components. (E) Calculate the Root Mean Square Error (RMSE) to assess the accuracy of the decomposition process. (F) Conduct a comparative analysis between Variational Mode Decomposition (VMD) and Continuous Wavelet Transform (CWT) for signal decomposition. (G) Generate a scalogram to visualize the time-frequency representation of the signal. (H) Create a coscalogram to display the co-contraction of TA-GL muscles.

The application of VMD denoising yields more reliable ankle-muscle sEMG signal enhancing the accuracy of subsequent co-contraction quantification. The novel combination of the Scalogram visualization technique with VMD is employed to gain insights into the time-frequency characteristics of the signal's intrinsic mode functions.

The co-scalogram results from Figs. 13 and 14 highlight periods of coordinated muscle activity, indicating co-contraction between antagonist muscles, and providing a visual representation of the temporal and frequency-specific aspects of this coordination. A coscalogram complements the information provided by individual scalograms of antagonistic muscle signals.

Panel A and B of Fig. 13 show the scalogram function of the sEMG signal, after VMD denoising, of antagonist muscles i.e. tibialis anterior (TA) and gastrocnemius lateralis (GL) respectively. Panel C shows a coscalogram of the cross-energy density in the time-frequency domain between the denoised TA and GL signals.

Discussion

This paper proposes a VMD method to characterize ankle muscle co-contraction in sEMG signal. To gain insights into the time-frequency characteristics of sEMG signals' intrinsic mode functions (IMFs), a novel combination of Scalogram visualization techniques is employed with VMD. The study focuses on the efficient denoising of the sEMG signal as a better-denoised signal will give a clear result of co-contraction that would be useful for the treatment of patients having ankle joint issues.

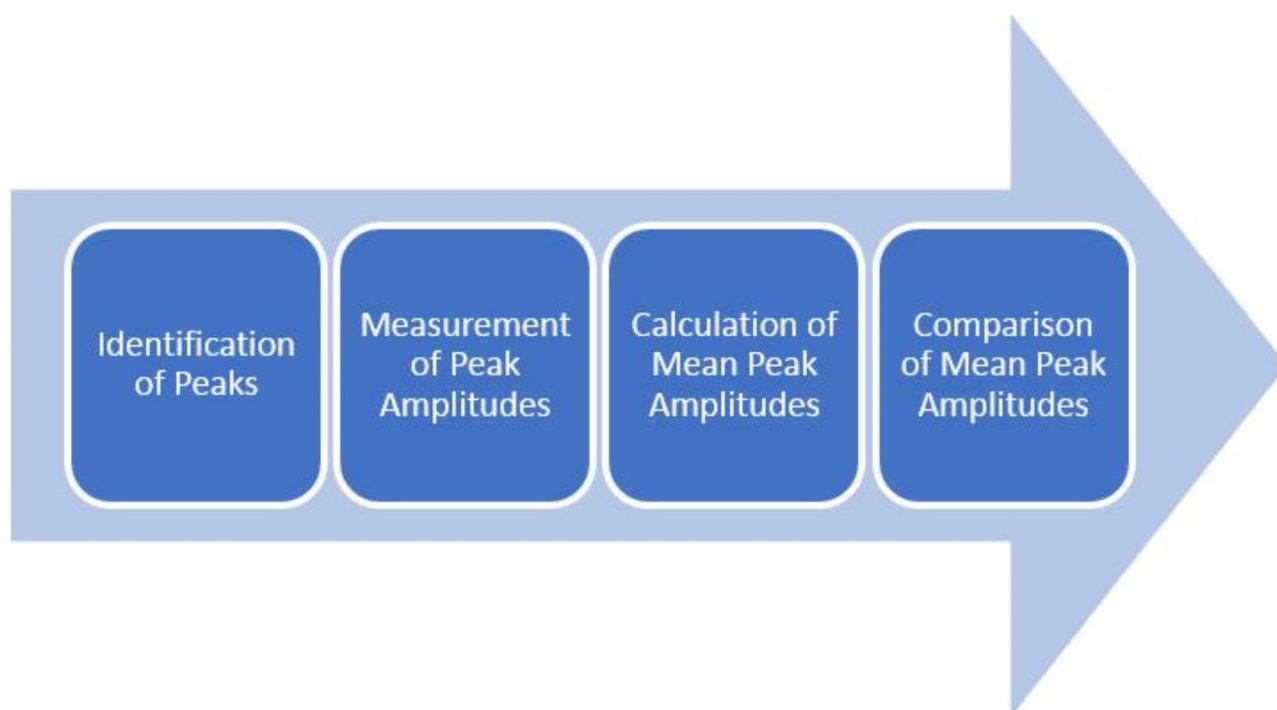


Fig. 5. Steps of quantitative assessment of co-contraction.

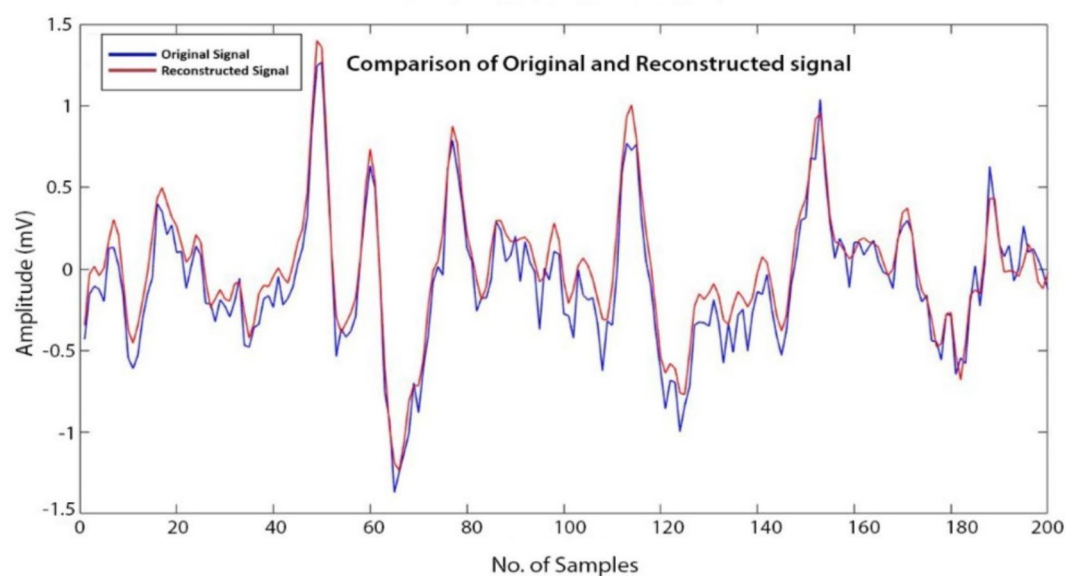


Fig. 6. Comparison between the original signal and the signal after denoising. The original sEMG signal contains high-frequency noise, which is effectively reduced through the applied denoising technique. The figure illustrates the effectiveness of the VMD in preserving the essential signal components while eliminating unwanted noise, ensuring a cleaner and more interpretable signal for further analysis.

Although CWT quantifies ankle muscles very finely as mentioned in³⁵, when VMD was compared with CWT by using online as well as offline data, the proposed method (VMD) provides better results than the previously proposed method (CWT) as evident from Figs. 11 and 12. In our study, we observed that, on average, the increase in SNR with VMD (from $-17.65 \pm 8.1\text{dB}$ to $2.98 \pm 2.2\text{dB}$, $p < 0.05$) exceeded that achieved with CWT (from $-17.65 \pm 3.7\text{dB}$ to $1.34 \pm 1.5\text{dB}$). Likewise, we found that the reduction in RMSE using VMD (from 0.023 ± 0.0029 to 0.017 ± 0.0015 , $p < 0.05$) outperformed CWT's performance (from 0.023 ± 0.0027 to 0.020 ± 0.0025). VMD, characterized by its iterative refinement of IMFs, shows superiority over CWT. The

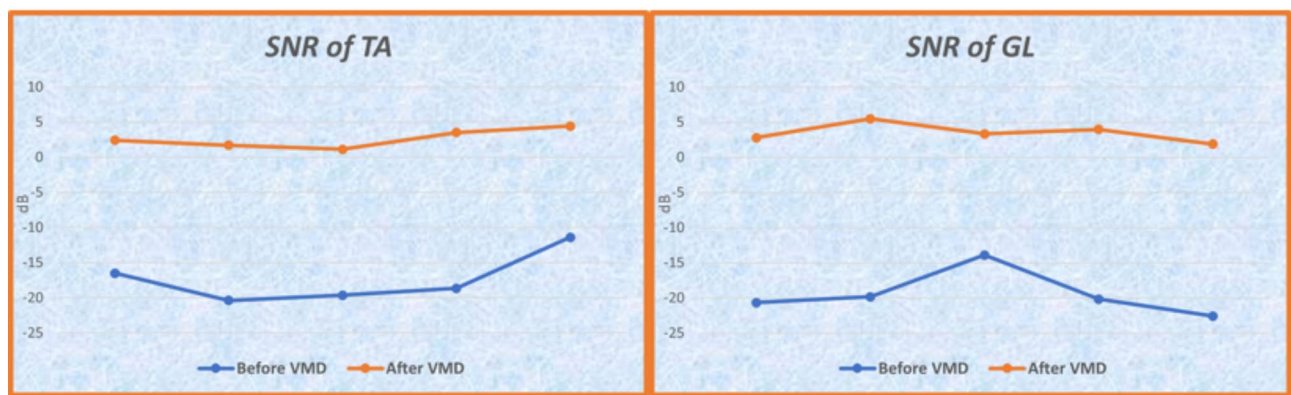


Fig. 7. SNR of TA and GL muscles before and after application of VMD.

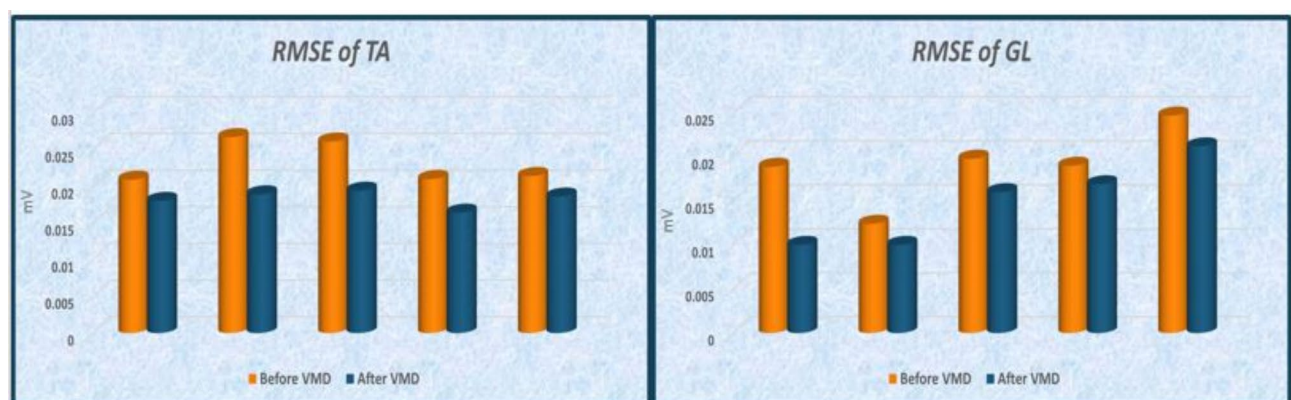


Fig. 8. RMSE of TA and GL muscles before and after application of VMD.

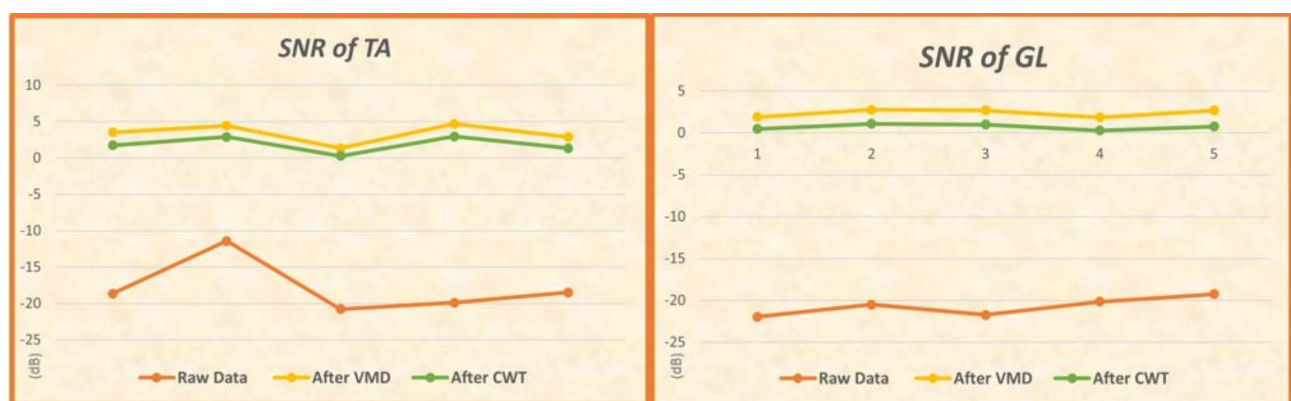


Fig. 9. Comparison of VMD and CWT in terms of SNR. A higher SNR indicates better noise reduction and signal preservation. The comparison highlights the effectiveness of VMD in enhancing signal quality compared to CWT.

single-pass nature of CWT limited its adaptability to complex signal environments, thereby rendering it less effective in achieving comparable levels of noise reduction.

Figure 6. clearly shows that denoising has been done effectively as the reconstructed signal maintains the attributes of the original signal. The reliability of the proposed method is proved by an increase in SNR in Fig. 7 and a decrease in RMSE in Fig. 8.

The identification of TA-GL co-contraction in Figs. 13 and 14 is achieved by analyzing the scalograms and coscalograms of the respective muscles. The scalogram of the TA muscle (Panel A) and the GL muscle

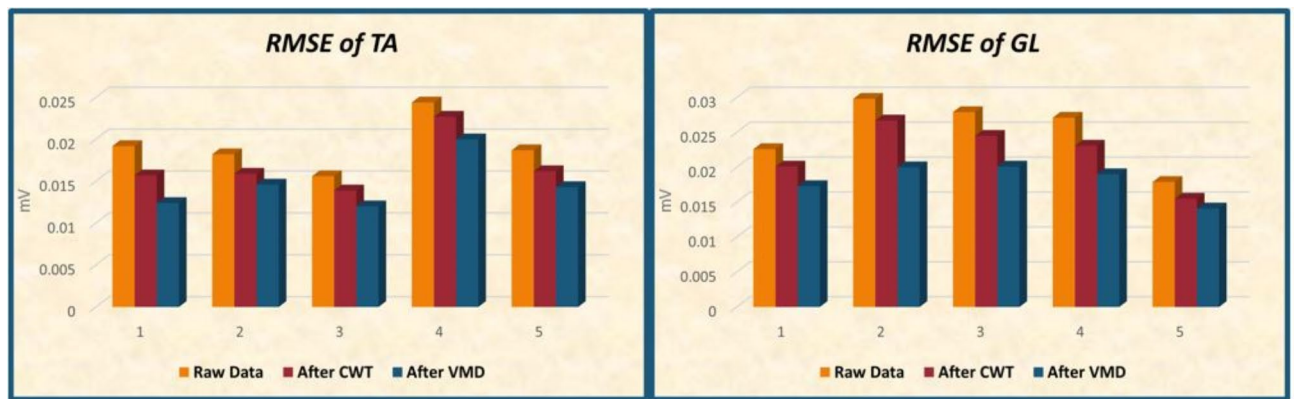


Fig. 10. Comparison of VMD and CWT in terms of RMSE. A lower RMSE indicates better signal reconstruction with minimal error. The comparison demonstrates the effectiveness of VMD in reducing reconstruction error compared to CWT.

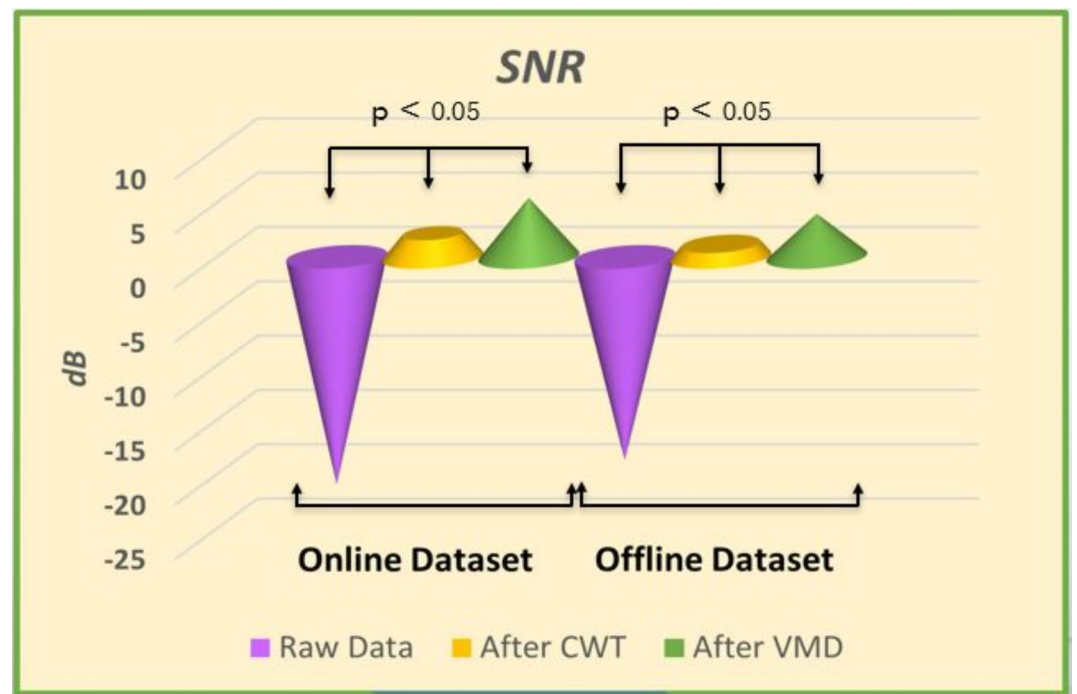


Fig. 11. Comparison of CWT and VMD using both online and offline datasets in terms of SNR.

(Panel B) individually display regions of muscle activation, indicated by yellow-colored areas, which represent high-intensity time-frequency components corresponding to muscle contraction. The coscalogram (Panel C) integrates the scalograms of both muscles, highlighting areas where simultaneous contraction occurs. Figures 13 and 14 shows that co-contraction of TA-GL will appear only on the coscalogram if both muscles contract at the same time. In Fig. 14, the right yellow box in panel C shows no co-contraction because the GL muscle is not activated, although TA shows activation. The left yellow box shows activation in panels A and B, so it also shows co-contraction in panel C. This visual representation allows for a clear identification of synchronized muscle activity and provides insights into the temporal characteristics of co-contraction between the TA and GL muscles.

The effectiveness of VMD and CWT was compared in detecting muscle co-contraction events by examining the mean peak amplitudes of co-scalograms. The results consistently showed that VMD produced higher mean peak amplitudes, suggesting stronger and more robust detection of co-contraction events. This quantitative assessment demonstrates the superior performance of VMD in capturing intense muscle activity, providing a clearer and more accurate representation of co-contraction dynamics compared to CWT.

While this study primarily compares VMD with CWT, other techniques such as Discrete Wavelet Transform (DWT), Empirical Mode Decomposition (EMD), and Sparse Representation Techniques have been widely used

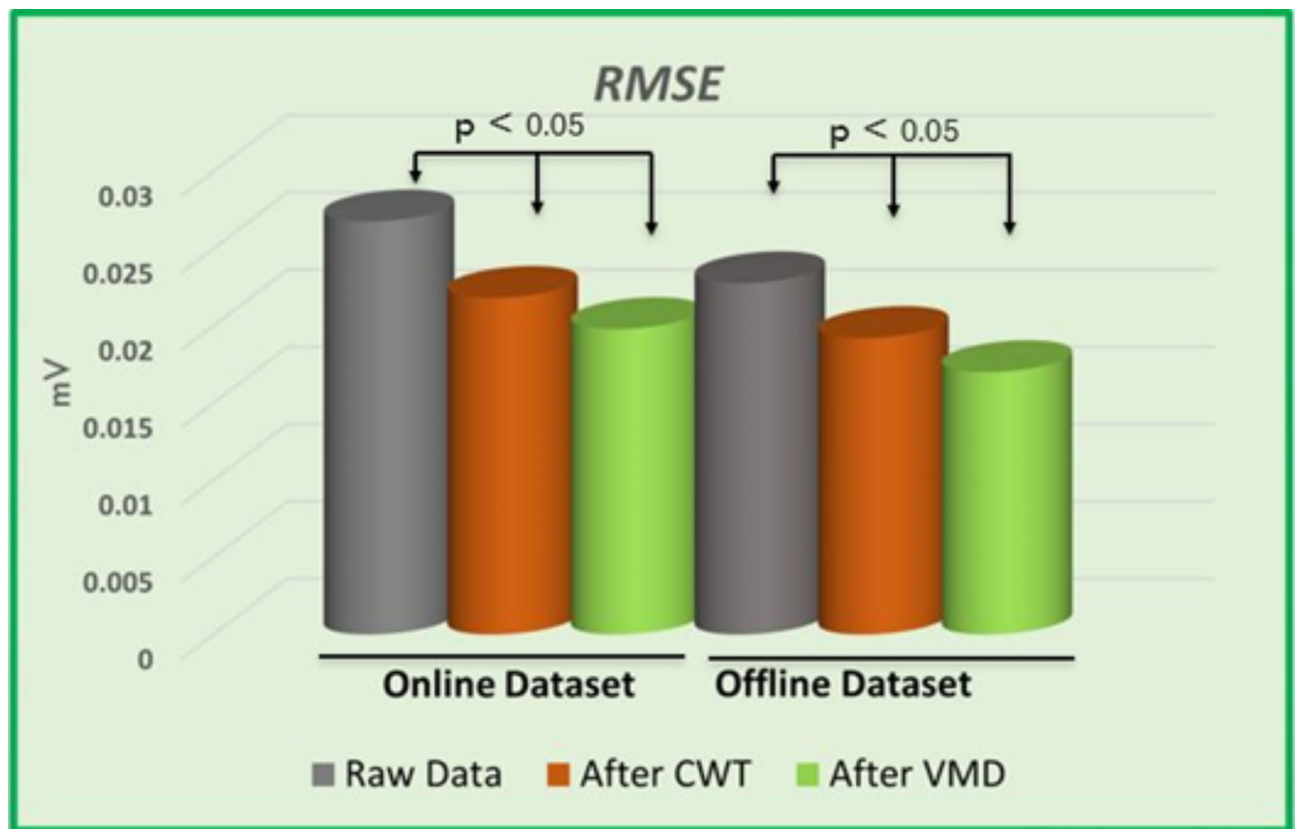


Fig. 12. Comparison of CWT and VMD using both online and offline datasets in terms of RMSE.

Serial No	Mean peak Amplitude (VMD)	Mean peak Amplitude (CWT)
1	2.284e-05	1.2e-05
2	3.142e-05	1.789e-05
3	2.876e-05	1.556e-05
4	3.500e-05	1.950e-05
5	2.950e-05	1.473e-05

Table 1. Mean peak amplitude values of VMD as well as CWT.

for EMG signal analysis. However, these methods present certain limitations: EMD suffers from mode-mixing issues, DWT lacks adaptive decomposition capabilities, and sparse representation methods require complex optimization models. In contrast, VMD provides improved mode separation and better adaptability to non-stationary signals, making it a more effective choice for muscle co-contraction analysis. Future research should explore these alternative methods to further validate the benefits of VMD.

Analyzing coscalograms provides insights into how different muscle groups work together to stabilize the ankle joint and ensure proper movement control, as cocontractions of ankle muscles play a pivotal role in maintaining joint stability. A coscalogram may help in assessing muscle coordination changes after injury and throughout the rehabilitation process. It aids clinicians and therapists in designing targeted exercises to restore optimal muscle cocontractions and joint stability.

Conclusion

The study aimed to detect and quantify the ankle muscle co-contraction accurately in sEMG signal for ankle rehabilitation purpose. The study proposes an efficient technique i.e., VMD to analyze surface electromyographic signals from TA-GL muscles of 20 healthy individuals and assess muscular co-contraction by using coscalogram function. This method (VMD) was compared with the previous used method (CWT) and the results prove that VMD provides better performance than CWT in terms of SNR and RMSE.

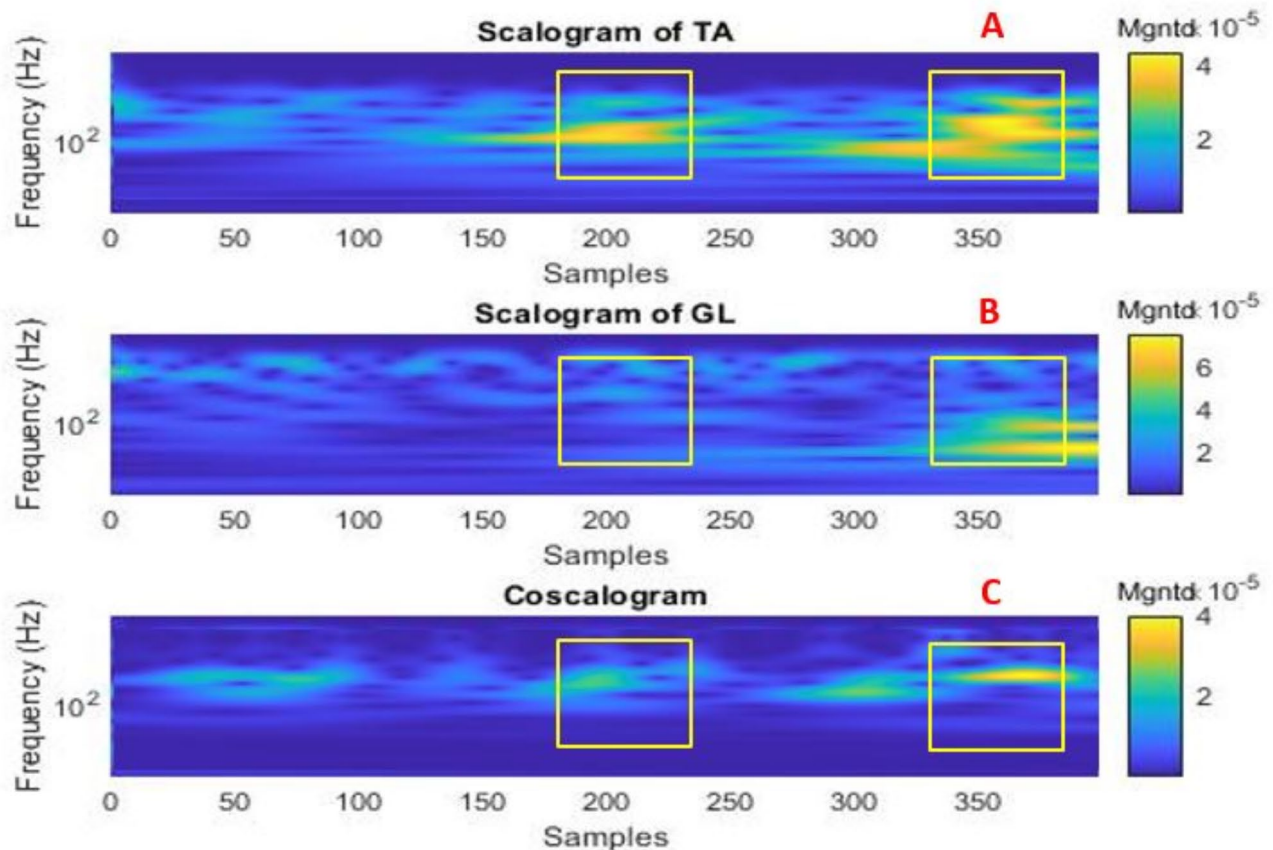


Fig. 13. Panel (A): TA sEMG Scalogram, Panel (B): GL sEMG Scalogram, Panel (C): TA-GL Coscalogram obtained by offline data.

Future recommendations

In future, investigation on the potential of incorporating machine learning techniques, such as deep learning or reinforcement learning, can be carried out to enhance the accuracy and real-time applicability of muscle co-contraction analysis in ankle rehabilitation. This study focused on the Tibialis Anterior (TA) and Gastrocnemius Lateralis (GL) muscles, which are key players in ankle function. However, other muscles, such as the soleus and peroneals, also contribute significantly to ankle stability and movement. The inclusion of these additional muscles would require specific protocol modifications, such as altered sensor placements and extended data acquisition periods, which were beyond the scope of the current study. Future research should investigate the co-contraction patterns of a broader muscle group to provide a more complete picture of ankle dynamics during walking. Including these additional muscles would enhance the clinical applicability of the proposed method. A key direction for future research is to investigate the co-contraction patterns in individuals with ankle pathologies (e.g., sprains, osteoarthritis, neurological conditions) which require specific ethical approvals. Investigating these populations is crucial for establishing the clinical utility of the proposed method and translating our findings into practical applications for rehabilitation. In cases where recruiting pathological subjects is challenging, data augmentation and generative AI-based techniques, such as those proposed by Yuan et al. (2023) and Trabassi et al. (2024), could potentially aid in creating synthetic datasets to simulate muscle co-contraction patterns in these populations. Future studies should also explore the impact of longer recording durations and more varied walking conditions on the analysis of muscle co-contraction. Including tasks such as walking on uneven surfaces or with added loads will help assess the method's robustness in more realistic and challenging environments.

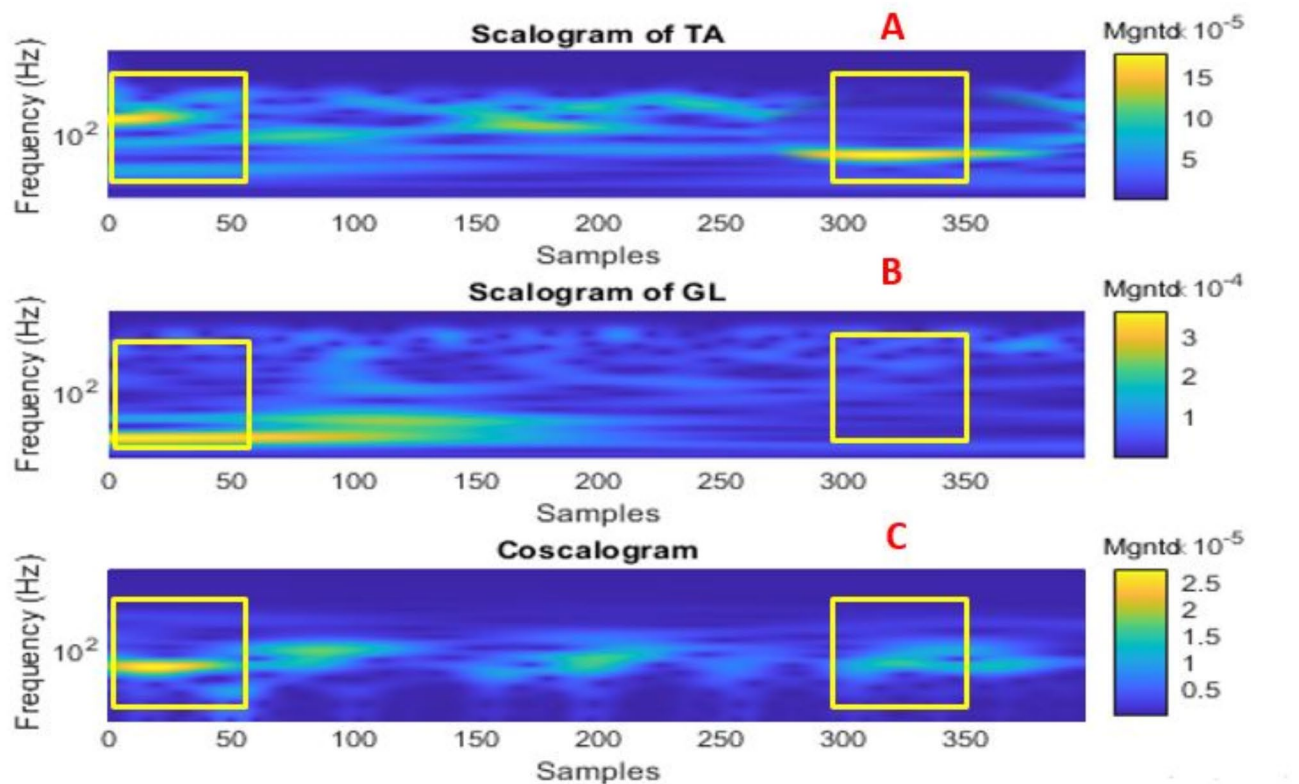


Fig. 14. Panel (A): TA sEMG Scalogram, Panel (B): GL sEMG Scalogram, Panel (C): TA-GL Coscalogram obtained by online data.

Data availability

Data sets generated during the current study are available from the corresponding author on reasonable request.

Received: 23 November 2024; Accepted: 27 March 2025

Published online: 28 April 2025

References

1. Zia ur Rehman, M. Z., Gilani, S. O., Waris, A., Niazi, I. K. & Kamavuako, E. N. A novel approach for classification of hand movements using surface EMG signals. in *IEEE International Symposium on Signal Processing and Information Technology (ISSPIT)* 265–269 (IEEE, 2017). (2017).
2. Farina, D. & Negro, F. Accessing the neural drive to muscle and translation to neurorehabilitation technologies. *IEEE Rev. Biomed. Eng.* **5**, 3–14 (2012).
3. Chowdhury, R. H. et al. Surface electromyography signal processing and classification techniques. *Sensors* **13**, 12431–12466 (2013).
4. Corcos, D. M., Gottlieb, G. L., Penn, R. D., Myklebust, B. & Agarwal, G. C. Movement deficits caused by hyperexcitable stretch reflexes in spastic humans. *Brain* **109**, 1043–1058 (1986).
5. Gohel, V. & Mehendale, N. Review on electromyography signal acquisition and processing. *Biophys. Rev.* **12**, 1361–1367 (2020).
6. Amin, F. et al. Maximizing stroke recovery with advanced technologies: A comprehensive review of robot-assisted, EMG-Controlled robotics, virtual reality, and mirror therapy interventions. *Results Eng.* **101725** (2023).
7. SH, R. & De Luca, C. J. Evolving characteristics of the median frequency of the EMG signal. *Computer-aided Electromyogr. Expert Syst.* 205–221 (1989).
8. Li, G., Shourijeh, M. S., Ao, D., Patten, C. & Fregly, B. J. How well do commonly used co-contraction indices approximate lower limb joint stiffness trends during gait for individuals post-stroke? *Front. Bioeng. Biotechnol.* **8**, 588908 (2021).
9. Knarr, B. A., Zeni Jr, J. A. & Higginson, J. S. Comparison of electromyography and joint moment as indicators of co-contraction. *J. Electromyogr. Kinesiol.* **22**, 607–611 (2012).
10. Den Otter, A. R., Geurts, A. C. H., Mulder, T. H. & Duysens, J. Abnormalities in the temporal patterning of lower extremity muscle activity in hemiparetic gait. *Gait Posture* **25**, 342–352 (2007).
11. Hallal, C. Z. et al. Lower limb muscle coactivation levels in healthy younger and older adults during functional dual-task gait. *Motriz: Revista De Educação Física*. **19**, 620–626 (2013).
12. Hortobágyi, T. et al. Interaction between age and gait velocity in the amplitude and timing of antagonist muscle coactivation. *Gait Posture*. **29**, 558–564 (2009).
13. Di Nardo, F., Morano, M., Strazza, A. & Fioretti, S. Muscle co-contraction detection in the time–frequency domain. *Sensors* **22**, 4886 (2022).
14. Rudolph, K. S., Axe, M. J. & Snyder-Mackler, L. Dynamic stability after ACL injury: Who can hop? *Knee Surg. Sports Traumatol. Art* **8**, 262–269 (2000).
15. Noor, A. et al. Decoding of ankle joint movements in stroke patients using surface electromyography. *Sensors* **21**, 1575 (2021).
16. Strazza, A. et al. Increased co-contraction activity during push-off phase of walking in healthy women. *IRBM* **42**, 48–54 (2021).

17. Mengarelli, A., Maranesi, E., Burattini, L., Fioretti, S. & Di Nardo, F. Co-contraction activity of ankle muscles during walking: A gender comparison. *Biomed. Signal Process. Control.* **33**, 1–9 (2017).
18. Panhan, A. C., Gonçalves, M. & Cardozo, A. C. Electromyographic activation and Co-contraction of the thigh muscles during pilates exercises on the Wunda chair. *J. Chiropr. Med.* **22**, 322–327 (2023).
19. Chaitanya, B. K., Yadav, A., Pazoki, M. & Abdelaziz, A. Y. A comprehensive review of islanding detection methods. *Uncertainties Mod. Power Syst.* 211–256 (2021).
20. Dragomiretskiy, K. & Zosso, D. Variational mode decomposition. *IEEE Trans. Signal Process.* **62**, 531–544 (2013).
21. Lian, J., Liu, Z., Wang, H. & Dong, X. Adaptive variational mode decomposition method for signal processing based on mode characteristic. *Mech. Syst. Signal Process.* **107**, 53–77 (2018).
22. Upadhyay, A. & Pachori, R. B. Instantaneous voiced/non-voiced detection in speech signals based on variational mode decomposition. *J. Franklin Inst.* **352**, 2679–2707 (2015).
23. Lahmiri, S. Comparative study of ECG signal denoising by wavelet thresholding in empirical and variational mode decomposition domains. *Healthc. Technol. Lett.* **1**, 104–109 (2014).
24. Li, F., Zhang, B., Verma, S. & Marfurt, K. J. Seismic signal denoising using thresholded variational mode decomposition. *Explor. Geophys.* **49**, 450–461 (2018).
25. Dora, C. & Biswal, P. K. An improved algorithm for efficient ocular artifact suppression from frontal EEG electrodes using VMD. *Biocybernetics Biomedical Eng.* **40**, 148–161 (2020).
26. Wang, Y., Markert, R., Xiang, J. & Zheng, W. Research on variational mode decomposition and its application in detecting rub-impact fault of the rotor system. *Mech. Syst. Signal Process.* **60**, 243–251 (2015).
27. Zhang, M., Jiang, Z. & Feng, K. Research on variational mode decomposition in rolling bearings fault diagnosis of the multistage centrifugal pump. *Mech. Syst. Signal Process.* **93**, 460–493 (2017).
28. Liu, W., Cao, S. & Chen, Y. Applications of variational mode decomposition in seismic time-frequency analysis. *GEOPHYSICS* **81**, V365–V378 (2016).
29. Liu, S. & Yu, K. Successive multivariate variational mode decomposition. *Multidim Syst. Sign Process.* **33**, 917–943 (2022).
30. Strazza, A. et al. Dynamic knee muscle co-contraction quantified during walking. in: *38th Annual International Conference of the IEEE Engineering in Medicine and Biology Society (EMBC)* 3692–3695 (IEEE, 2016). (2016).
31. Xiao, F., Yang, D., Guo, X. & Wang, Y. VMD-based denoising methods for surface electromyography signals. *J. Neural Eng.* **16**, 056017 (2019).
32. Liu, W., Liu, Y., Li, S. & Chen, Y. A review of variational mode decomposition in seismic data analysis. *Surv. Geophys.* **44**, 323–355 (2023).
33. Ashraf, H. et al. Variational mode decomposition for surface and intramuscular EMG signal denoising. *Biomed. Signal Process. Control.* **82**, 104560 (2023).
34. Di Nardo, F., Morano, M. & Fioretti, S. Quantification of ankle muscle co-contraction during early stance by wavelet-based analysis of surface electromyographic signals. in *IEEE International Symposium on Medical Measurements and Applications (MeMeA)* 1–5 (IEEE, 2022). (2022).
35. Hermens, H. J. et al. European recommendations for surface electromyography. *Roessingh Res. Dev.* **8**, 13–54 (1999).
36. Yuan, L., Yu, S., Yang, Z., Duan, M. & Li, K. A data balancing approach based on generative adversarial network. *Future Generation Comput. Syst.* **141**, 768–776 (2023).
37. Trabassi, D., Castiglia, S. F., Bini, F., Marinozzi, F., Ajoudani, A., Lorenzini, M., Serrao, M. (2024). Optimizing rare disease gait classification through data balancing and generative AI: Insights from hereditary cerebellar ataxia. *Sensors* **24**(11), 3613.

Author contributions

S. Yasmeen: conceptualization, investigation, methodology, validation, visualization, writing—original draft. A. Waris: Investigation, Methodology, Supervision, Validation, Writing—Review & Editing. F. Amin: Investigation, Validation, Visualization, Writing—review & editing. J. Iqbal: Validation, Visualization, Writing—review & editing. S.O. Gilani: Funding acquisition, software, supervision, validation, Writing—Review & editing. M.J. Khan: Funding acquisition, investigation, validation, writing—review & editing. F. Hazzazi: Funding acquisition, resources, validation, writing—review & editing. A. Imran: Funding acquisition, validation, visualization, writing—review & editing. U. H. Shah: Investigation, Methodology, Validation, Writing—Review & Editing. M. A. Ijaz: Methodology, Validation, Writing – review & editing.

Funding

This work was supported by the Abu Dhabi University ORSP grant (Grant number 19300909).

Declarations

Competing interests

The authors declare no competing interests.

Additional information

Correspondence and requests for materials should be addressed to M.J.K.

Reprints and permissions information is available at www.nature.com/reprints.

Publisher's note Springer Nature remains neutral with regard to jurisdictional claims in published maps and institutional affiliations.

Open Access This article is licensed under a Creative Commons Attribution-NonCommercial-NoDerivatives 4.0 International License, which permits any non-commercial use, sharing, distribution and reproduction in any medium or format, as long as you give appropriate credit to the original author(s) and the source, provide a link to the Creative Commons licence, and indicate if you modified the licensed material. You do not have permission under this licence to share adapted material derived from this article or parts of it. The images or other third party material in this article are included in the article's Creative Commons licence, unless indicated otherwise in a credit line to the material. If material is not included in the article's Creative Commons licence and your intended use is not permitted by statutory regulation or exceeds the permitted use, you will need to obtain permission directly from the copyright holder. To view a copy of this licence, visit <http://creativecommons.org/licenses/by-nc-nd/4.0/>.

© The Author(s) 2025